


Article

The Use of Geoinformatics in Coastal Atmospheric Transport Phenomena: The Athens Experiment

Theodoros Nitis ^{1,2,*}  and Nicolas Moussiopoulos ²¹ Laboratory of Environmental Quality and Geospatial Applications, Department of Marine Sciences, University of the Aegean, 81100 Mytilene, Lesbos, Greece² Laboratory of Heat Transfer and Environmental Engineering, Department of Mechanical Engineering, Aristotle University of Thessaloniki, 54124 Thessaloniki, Greece; moussio@eng.auth.gr

* Correspondence: theonitis@aegean.gr; Tel.: +30-22510-36822

Abstract: Coastal environment, an area where abrupt changes occur between land and sea, significantly affects the quality of life of a high portion of the Earth's population. Therefore, the wide range of phenomena observed in coastal areas need to be assessed reliably regarding both data sets and methods applied. In particular, the study of coastal atmospheric transport phenomena which affect a variety of activities in coastal areas, using modeling techniques, demand accurate estimations of a range of meteorological and climatological variables related to the planetary boundary layer. However, the accuracy of such estimations is not obvious. Geoinformatics is able to fill this gap and provide the framework for the design, processing and implementation of accurate geo-databases. This paper aims to highlight the role of geoinformatics in the context of coastal meteorology and climatology. More precisely, it aims to reveal the effect on the performance of a Mesoscale Meteorological Model when a new scheme regarding the input surface parameters is developed using satellite data and application of Geographical Information Systems. The development of the proposed scheme is described and evaluated using the coastal Metropolitan Area of Athens, Greece as a case study. The results indicate a general improvement in the model performance based on the statistical evaluations of three meteorological parameters (temperature, wind speed and wind direction) using four appropriate indicators. The best performance was observed for temperature, then for wind direction and finally for wind speed. The necessity of the proposed new scheme is further discussed.

Keywords: land-sea interaction; sea surface temperature; GIS; remote sensing; marine boundary layer; mesoscale meteorological models; aegean sea



Citation: Nitis, T.; Moussiopoulos, N. The Use of Geoinformatics in Coastal Atmospheric Transport Phenomena: The Athens Experiment. *J. Mar. Sci. Eng.* **2021**, *9*, 1197. <https://doi.org/10.3390/jmse9111197>

Academic Editor: Anabela Oliveira

Received: 13 September 2021

Accepted: 27 October 2021

Published: 29 October 2021

Publisher's Note: MDPI stays neutral with regard to jurisdictional claims in published maps and institutional affiliations.



Copyright: © 2021 by the authors. Licensee MDPI, Basel, Switzerland. This article is an open access article distributed under the terms and conditions of the Creative Commons Attribution (CC BY) license (<https://creativecommons.org/licenses/by/4.0/>).

1. Introduction

Land-sea interactions observed in coastal areas are quite complex and feed the appearance of phenomena falling within the scientific areas of climatology and meteorology at different spatio-temporal scales [1]. Air observation has always been an essential precondition for monitoring and predicting weather and studying the effects of climatic and meteorological phenomena [2]. In recent decades, the use of geoinformatics in a wide range of applications related to the climatic and meteorological data processing and analysis has increased [3–7]. Geoinformatics includes Geographical Information Systems (GIS) and remote sensing and uses information technologies for the collection, management, analysis, modeling and visualization of spatial data with the aim of assessing different phenomena and support relative decision-making [8,9].

In the fields of climatology and meteorology, GIS allow for a detailed analysis of different atmospheric parameters by providing specific information regarding weather and climate variability at different spatio-temporal scales [10]. In-situ meteorological observations and/or others acquired from satellite images provide a wide range of information stored in multiple thematic layers, which might be useful for a detailed description of the atmosphere state [11]. Furthermore, climatic and meteorological parameters are heavily

depended on factors such as topography, land use or vegetation type. The study of the spatio-temporal change of these parameters can be significantly facilitated within a GIS [12]. Spatial information can be stored in appropriate geo-databases in a GIS environment which may be very helpful in case of further update, synthesis, process, analysis, management and recovery of data sets. In addition, GISs allow the overlay of map layers from different sources, their geo-reference to a common coordinate system, and visualization of models' results [13]. Finally, the coupling of raw data and models on the earth-atmosphere interface is an important research topic that is facilitated in a GIS environment, particularly in terms of understanding air-sea interaction [14,15].

Satellite remote sensing is a key component of geoinformatics and is directly linked to GIS. Following the evolution of numerical prognostic models, satellite remote sensing has been considered as a very useful tool providing measurements of meteorological parameters at regular intervals and at different spatial scales [16]. It is important to note that the requirements of researchers regarding the modeling of atmospheric phenomena played an important role in the design of new missions of meteorological satellites. In addition to obtaining information for meteorological parameters, satellite remote sensing also provides valuable data on Earth surface parameters directly related to Earth-atmosphere interaction [17–21]. Furthermore, satellite remote sensing provides data on the radiation entering and leaving the earth-atmosphere system, whose spatio-temporal change is an important component of the atmosphere dynamics. The above parameters are input data for numerical models and their acquirement from high spatio-temporal resolution satellite sensors as well as their further processing and analysis in a GIS environment have contributed significantly to the improvement of models' performance [11].

The need of geoinformatics in meteorology and climatology has been widely recognized [22]; the European Union funded the COST719 Action in order to illustrate the use of GIS in the aforementioned fields and address the issue of spatial data management and distribution [3,12]. Furthermore, nowadays the improvements in these scientific fields have made available a wide spectrum of plugins for GIS which allow the performance of complete steps during model simulations [23]. Additionally, web-enabled geo-databases improve data use, since they provide quick and efficient access to information to various groups, supporting cost effective decision-making [24]. Finally, since satellite technology is evolving faster than numerical modeling, continuous update of numerical models is required in order to be benefited as much as possible from the enriched availability of satellite data sets [11].

The main objective of this paper was to extend and enhance the potential of geoinformatics in the field of mesoscale meteorological modeling. For this purpose, an Enhanced version of an existing Mesoscale Meteorological Model (MMM) was developed by integrating an accurate geo-database. The latter included surface parameters calculated from relevant satellite data using GIS analysis. The following steps were applied in order to fulfil this objective:

- Evaluation of the state-of-the-art of available geoinformatics tools and ongoing developments in progress;
- Evaluation of the accessibility and contents of available meteorological and other relevant data sets;
- Evaluation of the potential and restrictions of geoinformatics tools for spatialisation of necessary input data;
- Development of a new scheme regarding the surface parameters which is a joining mechanism between surface layer and the Atmospheric Boundary Layer (ABL).
- Development of an accurate geo-database that fulfills the needs of the surface parameters modification scheme.
- Evaluation of the performance of the Enhanced version for different time periods in a well-known study area which is a necessary and appropriate step to ensure the reliability of the new model version.

The study area is the Greater Athens Area, a coastal area with a dense urban fabric surrounded by mountains with only its southern part open to the sea. The area is influenced by both irregular topography and spatial variation of land surface characteristics representing therefore an ideal case for the evaluation of the enhanced version of the model. However, it should be noted here that the effect of topography on the model's performance is mostly indirect when the temperature and the wind speed/direction are considered. This impact will be clear in future work where the development and evolution of the Atmospheric Boundary Layer will be analysed.

2. Mesoscale Meteorological Model Enhanced Version

Detailed simulations of MMM under the influence of weak synoptic conditions are difficult to achieve. Surface parameters [1,19,25,26] play a dominant role on the comprehensive representation of local circulation systems in these models. In particular, accurate determination of thermophysical parameters is of high importance for the thermal (energy and radiation balance) and dynamical effects in the ABL. For this reason, analytical methodologies (e.g., Land Surface Models—LSM) were developed to describe the ABL in detail. However, there are still problems in the quantitative calculation of the required parameters [27] and many underestimations (e.g., in the calculation of temperature in coastal areas), which are associated with the insufficient representation of land-sea interaction [28]. In addition, it is necessary to investigate the necessity of complexity introduced in the models in order to achieve satisfactory parameterization of the surface layer, given the growing demand of MMM for operational applications [11]. Furthermore, application of complex parameterization requires the use of field data for many parameters at the mesoscale as well as at the microscale, which in most cases are very difficult to acquire [29].

Moreover, in a survey by Mölders [30] to analyze the uncertainty introduced to MMM by the surface parameters, it was concluded that it is preferable to use the actual values of these parameters if available, rather than values from reference tables resulting from matching land uses. In addition, Atkinson [31], in his attempt to analyze the effect of surface parameters on the urban heat island, noted that aerodynamic roughness and surface resistance to evaporation are the most important factors during the day, whereas man-made heat was important during the night. Furthermore, the impact of Sea Surface Temperature (SST) on the wind and air temperature in coastal areas are of significant importance affecting the local weather and climate [1,32,33]. The construction of an analytical geo-database regarding the aforementioned parameters from field data may be inaccurate or of high cost, thus being one of the most important limiting factors in the use of MMM. For this reason, the adaptation of biophysical parameters derived from satellite measurements with the use of geoinformatics is important for building geo-databases characterized by enhanced accuracy and high spatio-temporal resolution.

Based on the above mentioned, the Surface Parameter Modification Scheme (SPMS) was developed and introduced in a MMM in the framework of the Mesoscale Meteorological Model Enhanced Version (Figure 1). The basic characteristic of this scheme is the temporal and spatial variability of surface thermophysical parameters which are available for MMM applications. With the exception of anthropogenic heat, which was calculated based on the approach proposed by [34], the calculation of the remaining parameters (aerodynamic roughness, surface reflectivity, land and sea surface temperature, land-use and orography) was performed by processing of high-precision satellite data and application of relevant GIS techniques. The rest of the surface parameters involved (i.e., volumetric heat capacity) were determined using an updated MMM reference table [11]. Similar approaches to the proposed SPMS have been proposed by many research teams using different meteorological models. These approaches resulted in an improvement in the efficiency of MMMs by achieving a better description of the transport phenomena ([14,19,20,35]. The MMM Enhanced version proposed here aimed to reproduce in a realistic way the coastal transport phenomena, without using complex parameterizations which demand costly new datasets and excess computational time.

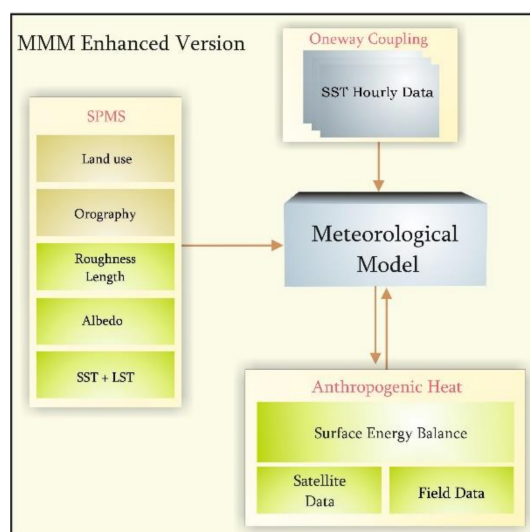


Figure 1. Schematic representation of the proposed Mesoscale Meteorological Model Enhanced Version.

3. Description of the Study Area and Model Setup

The Greater Athens Area (henceforth: GAA) was selected as case study (Figure 2—inner frame) for validating the proposed system, as it represents a prototypical example of a complex topographical configuration. The city of Athens is located in a basin of approximately 450 km (Figure 2), surrounded on three sides by fairly high mountains and open to the sea to the SW. In 2003, 3125 million people, approximately 28% of Greek population [36], lived in the Athens metropolitan area, which already suffers from air pollution problems.

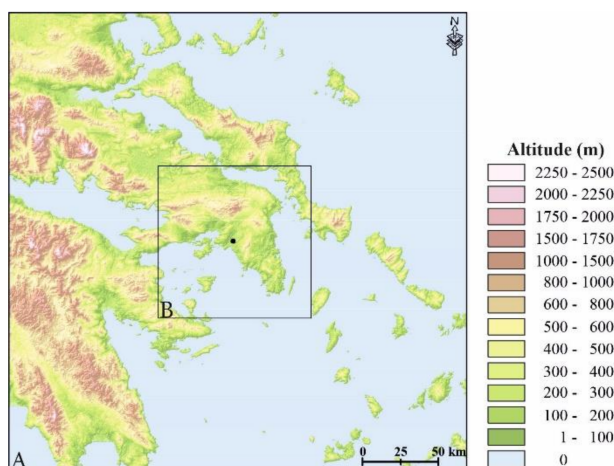


Figure 2. Configuration of nested grids. The outer frame (A) indicates the coarse grid ($300 \times 300 \text{ km}^2$), whereas the inner frame (B) indicates the fine grid ($100 \times 100 \text{ km}^2$). The bullet presents the center of both domains (Latitude $37^\circ 58' 4'' \text{ N}$, Longitude $23^\circ 44' 10'' \text{ E}$), 15 m above sea level.

Upper level charts (not shown here) for each studied period were considered; a high portion of Southern Europe (including investigated domain) was found to be within a high pressure field characterized by weak pressure gradients and consequent weak winds. It is widely known that such a weak synoptic leads to the development of local circulation systems, i.e., sea breeze, up- and down-slope winds and urban heat island-induced circulations. In this paper, an effort was made to account for all relevant orographic influences on the flow field. Therefore, based on the expanded radiation boundary condition, a nested system was adopted and the horizontal domain was extended so as to incorporate

a reasonable portion of land and sea masses [37]. The non-hydrostatic mesoscale model MEMO [14,38,39] was used for the simulation of wind and temperature fields for three multi-days periods: (a) 23–24 June 2002 (Period 1), (b) 29–30 June 2002 (Period 2) and (c) 19–20 September 2002 (Period 3), characterized by anticyclonic weather conditions.

The computational grid included 100×100 cells in the two horizontal directions and had a constant resolution of 1 km. In addition, the fine grid was provided by a coarse 300×300 km² mesoscale grid with a resolution of 3 km in a one-way coupled configuration and appropriate lateral conditions. The determination of the initial and boundary conditions of the coarse grid was performed using meteorological input information (vertical profiles of wind speed, wind direction and temperature) acquired from radiosondes data from the Athens airport station. Finally, an additional 24 h period was considered for each meteorological period as a spin-up period for the simulations.

4. Development of the Input Geo-Database

Mesoscale models require a wide range of input data that might have a quite high degree of uncertainty and could be difficult and costly to be collected. Geoinformatics, which include numerous remote sensing and GIS techniques for data collection and processing, provide a great advantage in this field; remote sensing data sets are of high spatial/temporal resolution and rich spectral content, cover extended areas and are available in various time scales. In this paper, a comprehensive input geo-database was developed using the advantages of geoinformatics. (1) The land use data set originated from the Corine land cover 2000 (CLC 2000) database [40], part of the European Commission programme to COoRdinate INformation on the Environment (Corine) and developed by the Topic Centre on Terrestrial Environment (ETC/TE). CLC 2000 Land Cover database includes 44 land cover types of about 100 m horizontal resolution. It should be noted here that in MEMO applications the original 44 land use types are reclassified into 7 more general ones. However, in the present paper, 11 general land use types were used since there was need for a more accurate representation of the urban environment. (2) The orography data set for the study area was acquired from the Shuttle Radar Topography Mission (SRTM) database [41]. It is one of the most complete high-resolution digital topographic databases of the Earth, with a horizontal grid of approximately 90 m, and was developed by the National Geospatial-Intelligence Agency (NGA) and the National Aeronautics and Space Administration (NASA).

(3) The accurate quantification of the aerodynamic roughness length (z_0), that is a crucial biophysical parameter, is of major importance, since it influences the energy exchange at the land-atmosphere interface. Several approaches for the estimation of z_0 at the regional scale are found in literature [42,43]. In this paper, simple empirical relationships between satellite radiometry and vegetation physiology were used for the calculation of the roughness length which concerned only non-artificial surfaces. Gupta et al. [44] and Moran et al. [45] described the linear relationship between z_0 and Normalized Difference Vegetation Index (NDVI) ($NDVI = \frac{NIR-RED}{NIR+RED}$ where *NIR* and *RED* are the radiances

in the Near InfraRed and Red spectral bands, respectively)), by the following formula:

$$z_0 = \exp(-5.5 + 5.8 \times NDVI) \quad (1)$$

The artificial surfaces are typically assigned a predefined value of z_0 , mostly based on the dominant land-use type. NDVI values were derived from MODIS satellite data and the z_0 value was calculated separately for each time period (June, July and September 2002) because of its strong dependence on seasonal variations.

(4) Land surface albedo is an important modulator of the surface energy budget representing the fraction of incident radiation reflected by a surface. However, in modelling attempts this parameter is characterized by a high degree of uncertainty, since models commonly prescribe albedo using in-situ observations, which are frequently sparse at a

regional scale [46]. In this paper, the MODIS/Terra-Aqua albedo 16 day, 1 km product was used (Figure 3) and in particular, the black-sky albedo (at local solar noon) for three broad bands (0.3–0.7 μm , 0.7–5.0 μm and 0.3–5.0 μm); the wavelengths 0.3–5.0 μm affect the surface energy balance. Black-sky albedo (α_{bs}) is defined as the albedo in the absence of a diffuse component and is a function of solar zenith angle [47]. The α_{bs} was used here because it is relatively close to the actual albedo, since it represents the integration of the α_{bs} over all solar zenith angles [47].

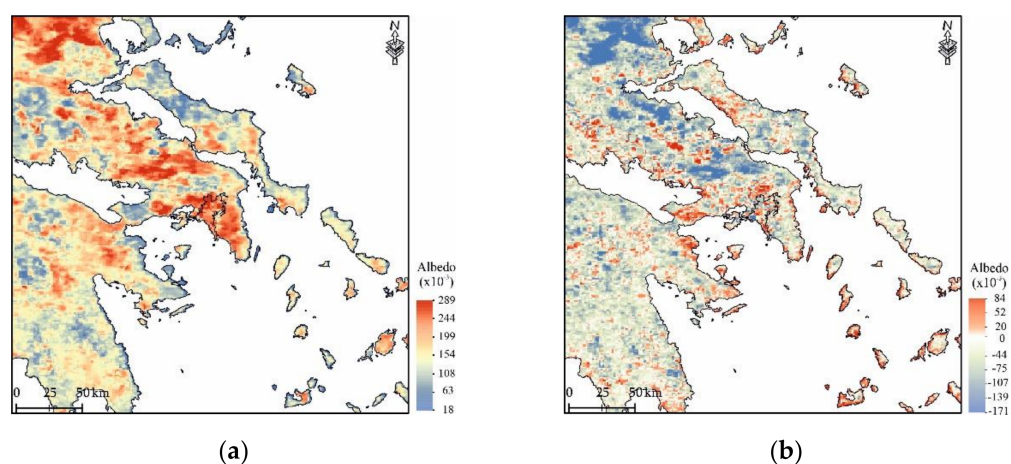


Figure 3. (a) Spatial distribution of average albedo from 26 June 2002 to 11 July 2002; (b) Spatial change of 16 days average albedo between the periods starting on 26 June 2002 and on 14 September 2002.

(5) Initial night time Land and Sea Surface Temperatures (LST and SST) over the study area were acquired from the Moderate-resolution Imaging Spectro-radiometer (MODIS) instruments aboard the NASA Terra and Aqua satellites [8,9]. The inputs included daily LST and SST composites with a spatial resolution of 1 km and 4 km, respectively. However, the data was converted to 8 day composites to reduce the presence of cloud shadows, since the inclusion of pixels within areas of cloud shadow was possible. The detailed hourly SST fields were acquired from the POSEIDON system operated by the Hellenic Centre for Marine Research; from 18 UTC 27 June 2002 to 18UTC 1 July 2002 and from 18 UTC 17 September 2002 to 18 UTC 21 September 2002. Further data processing with the use of geoinformatics was performed to ensure that the data were properly formatted. Results of the spatial distribution of the week average night surface temperature for the period 16–23 September 2002, as well as the difference of SST values between 12:00 and 24:00 for the 28th of June 2002 are shown in Figure 4.

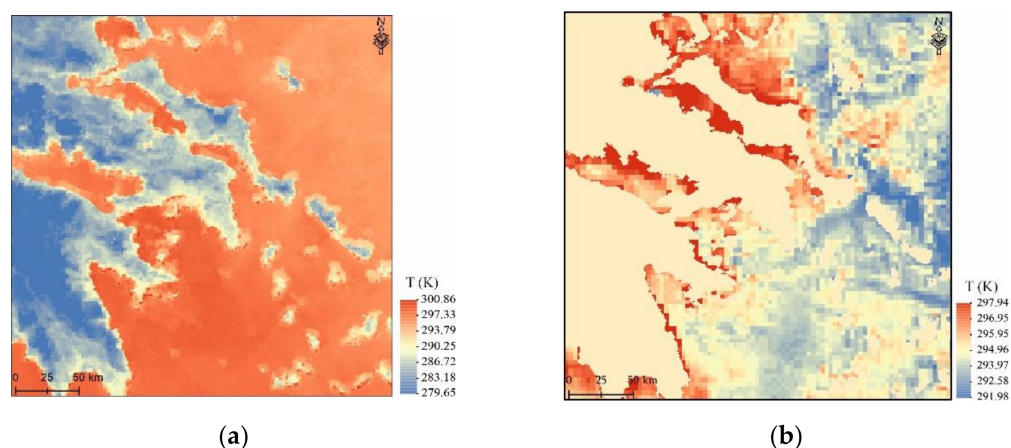


Figure 4. (a) Spatial distribution of the (α) week average night LST and SST for the period 16–23 September 2002; (b) difference of SST values between 12:00 and 24:00 for the 28th of June 2002.

(6) Waste heat generated from human activities and emitted to the ABL represents a parameter known as Anthropogenic Heat Flux (Q_f) which is one of the most important surface parameters for MMM and impacts ABL [48]. This flux varies significantly both in time and space, and is not readily measured or calculated. In particular, in urban areas, Q_f is difficult to be quantified directly and accurately. In this paper, the anthropogenic heat discharge in the GAA was estimated based on the urban canopy energy balance equation and use of combined advanced space borne thermal emission and reflection radiometer remote-sensing data and ground meteorological data [11,49]. The results are shown in Figure 5 for typical summer days with a spatial resolution of 30 m.

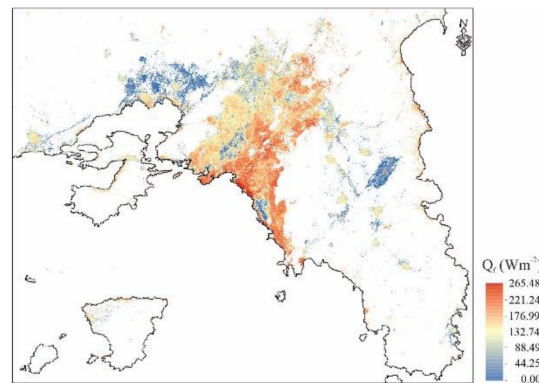


Figure 5. Spatial distribution of the anthropogenic heat for the Greater Athens Area for 26 July 2001.

5. Model Evaluation Results

The performance of the MEMO model was assessed and the Initial version (Iver) was compared to the Enhanced one. It should be noted here that the diurnal SST data as well as the anthropogenic heat data were excluded from this process, since the performance of the model should be tested using similar parameterizations regarding the Initial and the Enhanced versions [11]; therefore, the version compared to Iver was the SPMS (SPMSver). In addition, in order to achieve the highest credibility of the evaluation, the maximum possible field information was collected from a reliable network of meteorological stations in the study area. More specifically, information was collected from 17 meteorological stations; their locations are presented in Figure 6. The data sets were acquired from the Ministry of the Environment and Energy, the Athens International Airport, the National Observatory of Athens and the Development Association of the Thriasion Plain Municipalities.

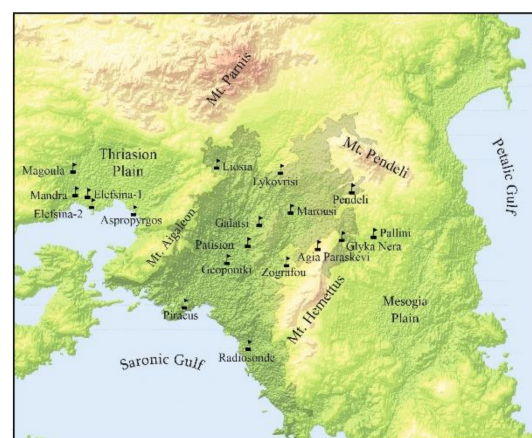


Figure 6. Spatial distribution of the routine measuring sites in the Greater Athens Area. The shadowed area represents the Athens Metropolitan Area.

The model performance was assessed by calculating the (i) Mean Bias Error (MBE), (ii) Mean Absolute Error (MAE) and (iii) Root Mean Square Error (RMSE), which represents

the average error produced by the model, and (iv) the index of agreement (d), which determines the degree of agreement between the observed and simulated values [50]. The values of d vary between 0.0, when there is no agreement between the observed and the predicted values, and 1.0, which represents a perfect agreement between the observed and the predicted values [51]. Therefore, to obtain a good prediction the value of d should be close to 1.0 and the value of errors close to 0.0. The evaluation of the results for the GAA showed that for all meteorological periods and for the three parameters under study (wind speed and direction, and temperature) the model simulated the reality reasonably well, while there is a quite important improvement in the performance of the SPMSver compared to the Iver.

5.1. Wind Speed

In Figure 7 the index of agreement for the two versions of MEMO and the three meteorological periods is illustrated. For the Iver, the index of agreement ranged from 0.534 to 0.690, while for the SPMSver it ranged from 0.592 to 0.718 indicating an improvement for all three meteorological periods; the latter was significant especially for Periods 1 and 3. It is also noted that the index of agreement was greater than 0.5 for all periods in both versions. In conclusion, the SPMSver improved the model results with the best performance observed in Period 2.



Figure 7. Illustration of the medians of the index of agreement values for the wind speed of the Iver (in blue) in comparison to the SPMSver (in orange) for the three meteorological periods.

In Table 1 the values of the statistical indicators calculated for the three meteorological periods are shown. For the Iver the RMSE ranged from 1.415 to 2.225 ms^{-1} , while for the SPMSver it ranged from 1.297 to 1.666 ms^{-1} and showed a decrease for all three meteorological periods with the larger one for Period 1. In general, there is an improvement in the results of the model with the best performance observed for Periods 2 and 3. The MAE ranged from 1.111 to 1.749 ms^{-1} for the Iver, while for the SPMSver it ranged from 1.051 to 1.347 ms^{-1} and showed a decrease for all three meteorological periods with the larger one for Period 1. The MBE ranged from -0.380 to 0.839 ms^{-1} for the Iver, while for the SPMSver it ranged from -0.646 to 0.874 ms^{-1} . In Period 2 the model had the best performance; while it overestimated the reality in both versions, this overestimation was reduced in the SPMSver.

Table 1. Median values of MBE, MAE, RMSE and d for the Iver and SPMSver and the three meteorological periods regarding wind speed (ms^{-1}).

	Iver				SPMSver			
	MBE	MAE	RMSE	d	MBE	MAE	RMSE	d
Period 1	−0.380	1.749	2.225	0.534	−0.646	1.347	1.666	0.592
Period 2	0.670	1.215	1.457	0.690	0.483	1.051	1.370	0.718
Period 3	0.839	1.111	1.415	0.577	0.874	1.075	1.297	0.617

5.2. Wind Direction

In Figure 8, the index of agreement for the two versions of MEMO and the three meteorological periods is presented. For the Iver the index of agreement ranged from 0.753 to 0.809, while for the SPMSver it ranged from 0.765 to 0.838 and showed an increase for all three meteorological periods. The greater improvement was observed for Period 1. The above indicated an improvement of the model's performance in the SPMSver.



Figure 8. Illustration of the medians of the index of agreement values for the wind direction of the Iver (in blue) in comparison to the SPMSver (in orange) for the three meteorological periods.

In Table 2 the values of the statistical indicators calculated for the three meteorological periods are shown. RMSE ranged from 75.6 to 91.7 deg for the Iver, while for the SPMSver it ranged from 78.0 to 85.7 deg with the better performance observed for Period 2. MAE ranged for the Iver from 58.3 to 73.1 deg, while for the SPMSver it ranged from 58.8 to 65.2 deg with the better performance also observed for Period 2. The MBE ranged from −30.1 to 22.6 deg for the Iver, while for the SPMSver it ranged from −31.6 to 8.1 deg. The lowest value appeared for Period 1.

Table 2. Median values of MBE, MAE, RMSE and d for the Iver and SPMSver and the three meteorological periods regarding wind direction.

	Iver				SPMSver			
	MBE	MAE	RMSE	d	MBE	MAE	RMSE	d
Period 1	22.6	73.1	91.7	0.809	8.1	58.8	79.1	0.838
Period 2	−30.1	58.3	75.6	0.763	−31.6	59.5	78.0	0.779
Period 3	−7.2	63.2	77.6	0.753	−15.3	65.2	85.7	0.765

For all meteorological periods, the highest index of agreement (>0.86) for the SPMSver was observed at the stations of Liossia (0.850) and Maroussi (0.816). The lowest value of RMSE and MAE was observed for all three periods at the Lykovrysi station. Regarding MBE, the lowest values were observed at the stations located in Thriasio Pedio for all meteorological periods and more specifically at Elefsina-1 (1.745 deg) for Period 1, Elefsina-2 (1.939 deg) and Mandra (1.414 deg) for Period 2 and Magoula (9.862 deg) for Period 3. These values indicated an overestimation of reality by the model as a whole.

5.3. Temperature

In Figure 9 the index agreement for the two versions of MEMO and the three meteorological periods is presented. For the Iver, the index of agreement ranged from 0.737 to 0.903, while for the SPMSver it ranged from 0.835 to 0.925 and showed an increase for all three meteorological periods. The greater improvement was observed for Period 1, while the index of agreement for the SPMSver was above 0.8 for all periods. As a result, an improvement of the results in the SPMSver with the best performance for Period 2 was observed.

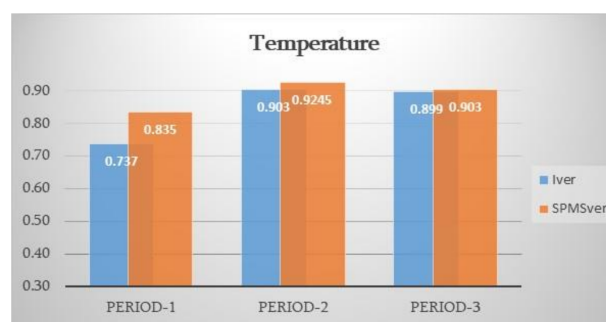


Figure 9. Illustration of the medians of the index of agreement values for the Temperature of the Iver (in blue) in comparison to the SPMSver (in orange) for the three meteorological periods.

In Table 3 the values of the statistical indicators calculated for the three meteorological periods are shown. RMSE ranged for the Iver from 1.819 to 2.827 °K, while for the SPMSver it ranged from 1.837 to 2.512 °K. The MAE ranged for the Iver from 1.548 to 2.285 °K, while for the SPMSver it ranged from 1.553 to 2.033 °K. The best performance of the model in terms of RMSE (1.837 °K) and MAE (1.553 °K) values for the SPMSver was observed for Period 2. MBE ranged from -0.311 to 0.908 °K for the Iver, while for the SPMSver it ranged from 0.097 to 0.379 °K. For the SPMSver there was an overestimation of reality from the model for all meteorological periods with the shortest observed for Period 3. For all meteorological periods, the highest index of agreement (>0.80) for the SPMSver was observed at the stations of Liossia, Lykovrysi and Maroussi. The lowest values of RMSE, MAE and MBE were observed for all three periods at the stations of Liossia and Maroussi with overestimation of reality by the model.

Table 3. Median values of MBE, MAE, RMSE and d for the Iver and SPMSver and the three meteorological periods regarding temperature (°K).

	Iver				SPMSver			
	MBE	MAE	RMSE	d	MBE	MAE	RMSE	d
Period 1	−0.311	2.285	2.827	0.737	0.378	2.033	2.512	0.835
Period 2	−0.040	1.655	2.006	0.903	0.379	1.553	1.837	0.925
Period 3	0.908	1.548	1.819	0.899	0.097	1.790	2.111	0.903

The general conclusion is that for both versions the performance was generally good and the model managed to simulate the reality reasonably well, especially for temperature. In particular, the SPMSver produced better results, especially for the first period studied. In Table 4, the differences between the SPMSver and Iver regarding the statistical indicators are presented; the MBE due to its nature was excluded since it cannot give relevant information in this kind of analysis. Furthermore, it should be mentioned that both versions' performance was relatively high and for this reason in some cases the differences in the values of the statistical indicators between the two versions are not so high. For instance, for Period 2 the index of agreement (d) for temperature reached values close to perfect agreement (Table 3) and the 2.2% improvement shown in Table 4, though low as a value (0.022), corresponds to a positive trend of improvement of the model performance.

Table 4. The amount of difference of the four statistical indicators' values between the SPMSver and the Iver.

	Wind Speed			Wind Direction			Temperature		
	MAE	RMSE	d	MAE	RMSE	d	MAE	RMSE	d
Period 1	−0.402	−0.560	0.057	−14.27	−12.57	0.028	−0.252	−0.315	0.098
Period 2	−0.164	−0.087	0.028	1.19	2.31	0.016	−0.102	−0.170	0.022
Period 3	−0.036	−0.118	0.040	1.99	8.13	0.012	0.242	0.292	0.004

Overall, a satisfactory performance of the model was detected, as it is able to reproduce the structure and the evolution of the atmospheric boundary layer in the coastal area of Athens. As mentioned above, the main aim of this work was the evaluation of the new surface scheme which is a pre-requisite for a consequent analysis of the land–sea interaction and relevant transport phenomena, which includes the impact of the complex terrain on the local circulation patterns as well as the vertical structure of the marine boundary layer.

6. Conclusions

In this paper, the need for comprehensive prognostic meteorological models related to environmental assessment along with their demand for incorporating the complex interactions related to the dynamical and thermal effects of the surface layer are addressed. The emphasis was put on an Enhanced version of MMM which was developed focusing on the improvement of the surface parameters. The latter was achieved taking advantage (i) of the availability of various data sets from satellite images at different spatio-temporal scales and (ii) of the fact that many climatological and meteorological parameters depend strongly on factors, such as land-use, vegetation species or building height etc., that their spatial and/or temporal changes can be analyzed easily and accurately using geoinformatics. The application of the SPMSver proved able to improve the MEMO performance. An important characteristic of the new scheme is that it is based on freely available data (via internet) with a spatial and temporal variability with satisfactory performance and computational time demand. As far as the developed geo-database is concerned, it can be easily updated and expanded in a GIS and therefore be useful in many other cases.

It is noteworthy to mention that the spatial resolution of the input data sets was significantly higher than the model's finest resolution ($1 \times 1 \text{ km}^2$) used. Generally, the prediction of any MMM which uses high resolution data sources for its surface parameterizations is limited by the assumptions made by parameterization; for example, how the meteorological model's resolution and definition of the local terrain features influence the calculation of the low-level wind field [52,53]. Moreover, the analysis made in Section 5 clearly shows that using high resolution thermophysical parameters' data improves the results of calculating wind speed and direction and temperature on $1 \times 1 \text{ km}^2$. More precisely, according to [54] the overall performance of the SPMSver was good for all parameters for all three meteorological periods ($d \geq 0.592$). The best performance was observed for temperature, then for wind direction and finally for wind speed. It has to be mentioned that this approach (SPMSver) has been also applied to another case study in the past. The results of both studies indicated an encouraging model performance for providing useful forecasts of the local transport phenomena in coastal zone.

In general, the implementation of such geo-databases seems to significantly increase the productivity of scientific groups who spend the majority of their working time to prepare data sets in appropriate formats, indicating the necessity of geoinformatics in numerical model prediction.

Author Contributions: Conceptualization, T.N. and N.M.; methodology, T.N.; software, T.N. and N.M.; validation, T.N. and N.M.; investigation, T.N.; resources, T.N.; data curation, T.N.; writing—original draft preparation, T.N.; writing—review and editing, T.N. and N.M.; visualization, T.N.; supervision, N.M. All authors have read and agreed to the published version of the manuscript.

Funding: This research received no external funding.

Institutional Review Board Statement: Not applicable.

Informed Consent Statement: Not applicable.

Data Availability Statement: Not applicable.

Conflicts of Interest: The authors declare no conflict of interest.

References

- Dragaud, I.C.D.A.V.; Soares da Silva, M.; Assad, L.P.D.F.; Cataldi, M.; Landau, L.; Elias, R.N.; Pimentel, L.C.G. The impact of sst on the wind and air temperature simulations: A case study for the coastal region of the rio de janeiro state. *Meteorol. Atmos. Phys.* **2019**, *131*, 1083–1097. [\[CrossRef\]](#)
- Kidd, C.; Levizzani, V.; Bauer, P. A review of satellite meteorology and climatology at the start of the twenty-first century. *Progress Phys. Geogr.* **2009**, *33*, 474–489. [\[CrossRef\]](#)
- Thornes, J.; Dyras, I.; Wilhelmi, O. Special issue on the use of gis in climatology and meteorology. *Meteorol. Appl.* **2005**, *12*, 1–3. [\[CrossRef\]](#)
- Kotta, D.; Kitsiou, D. Exploring possible influence of dust episodes on surface marine chlorophyll concentrations. *J. Mar. Sci. Eng.* **2019**, *7*, 50. [\[CrossRef\]](#)
- Kotta, D.; Kitsiou, D. Medicanes triggering chlorophyll increase. *J. Mar. Sci. Eng.* **2019**, *7*, 75. [\[CrossRef\]](#)
- Karagulian, F.; Temimi, M.; Ghebreyesus, D.; Weston, M.; Kondapalli, N.K.; Valappil, V.K.; Aldababesh, A.; Lyapustin, A.; Chaouch, N.; Al Hammadi, F.; et al. Analysis of a severe dust storm and its impact on air quality conditions using wrf-chem modeling, satellite imagery, and ground observations. *Air Qual. Atmos. Health* **2019**, *12*, 453–470. [\[CrossRef\]](#)
- Gohain, K.J.; Mohammad, P.; Goswami, A. Assessing the impact of land use land cover changes on land surface temperature over pune city, India. *Quat. Int.* **2021**, *575–576*, 259–269. [\[CrossRef\]](#)
- Ehlers, M. Geoinformatics and digital earth initiatives: A german perspective. *Int. J. Digit. Earth* **2008**, *1*, 17–30. [\[CrossRef\]](#)
- Habermann, T. What is gis (for unidata)? *Bull. Am. Meteorol. Soc.* **2005**, *86*, 174–175. [\[CrossRef\]](#)
- Armstrong, L. *Mapping and Modeling Weather and Climate with Gis*; Esri Press: Redlands, CA, USA, 2014; pp. 1–370.
- Nitis, T. *An Atmospheric Environment Management System Incorporating the Impact of Urban Areas and Using Geoinformatics*; Aristotle University Thessaloniki: Thessaloniki, Greece, 2016; p. 191.
- Dyras, I.; Dobesch, H.; Grueter, E.; Perdigao, A.; Tveito, O.E.; Thornes, J.E.; Wel, F.; Bottai, L. The use of geographic information systems in climatology and meteorology: Cost 719. *Meteorol. Appl.* **2005**, *12*, 1–5. [\[CrossRef\]](#)
- Coutu, S.; Wyrsh, V.; Rossi, L.; Emery, P.; Golay, F.; Carneiro, C. Modelling wind-driven rain on buildings in urbanized area using 3-d gis and lidar datasets. *Build. Environ.* **2013**, *59*, 528–535. [\[CrossRef\]](#)
- Nitis, T.; Klaic, Z.B.; Kitsiou, D.; Moussiopoulos, N. Meteorological simulations with use of satellite data for assessing urban heat island under summertime anticyclonic conditions. *Int. J. Environ. Pollut.* **2010**, *40*, 123–135. [\[CrossRef\]](#)
- Fonseca, R.; Zorzano-Mier, M.-P.; Azua-Bustos, A.; González-Silva, C.; Martín-Torres, J. A surface temperature and moisture intercomparison study of the weather research and forecasting model, in-situ measurements and satellite observations over the atacama desert. *Q. J. R. Meteorol. Soc.* **2019**, *145*, 2202–2220. [\[CrossRef\]](#)
- Thies, B.; Bendix, J. Satellite based remote sensing of weather and climate: Recent achievements and future perspectives. *Meteorol. Appl.* **2011**, *18*, 262–295. [\[CrossRef\]](#)
- Hasager, C.B.; Jensen, N.O. Surface-flux aggregation in heterogeneous terrain. *Q. J. R. Meteorol. Soc.* **1999**, *125*, 2075–2102. [\[CrossRef\]](#)
- Schadlich, S.; Gottsche, F.M.; Olesen, F.S. Influence of land surface parameters and atmosphere on meteosat brightness temperatures and generation of land surface temperature maps by temporally and spatially interpolating atmospheric correction. *Remote Sens. Environ.* **2001**, *75*, 39–46. [\[CrossRef\]](#)
- De Foy, B.; Molina, L.T.; Molina, M.J. Satellite-derived land surface parameters for mesoscale modelling of the mexico city basin. *Atmos. Chem. Phys.* **2006**, *6*, 1315–1330. [\[CrossRef\]](#)
- De Meij, A.; Vinuesa, J.F. Impact of srtm and corine land cover data on meteorological parameters using wrf. *Atmos. Res.* **2014**, *143*, 351–370. [\[CrossRef\]](#)
- Temimi, M.; Fonseca, R.; Nelli, N.; Weston, M.; Thota, M.; Valappil, V.; Branch, O.; Wizemann, H.; Kondapalli, N.K.; Wehbe, Y.; et al. Assessing the impact of changes in land surface conditions on wrf predictions in arid regions. *J. Hydrometeorol.* **2020**, *21*, 2829–2853. [\[CrossRef\]](#)
- Shipley, S.T. Gis applications in meteorology, or adventures in a parallel universe. *Bull. Am. Meteorol. Soc.* **2005**, *86*, 171–173. [\[CrossRef\]](#)
- Steenefeld, G.J.; Vilà-Guerau de Arellano, J. Teaching atmospheric modeling at the graduate level: 15 years of using mesoscale models as educational tools in an active learning environment. *Bull. Am. Meteorol. Soc.* **2019**, *100*, 2157–2174. [\[CrossRef\]](#)
- Umphlett, N.A.; Pettee, W.; Sorensen, W.; Stiles, C.J. Enhancing acis maps: Increasing usability through a gis portal. *Bull. Am. Meteorol. Soc.* **2019**, *100*, 2417–2421. [\[CrossRef\]](#)
- Hembree, G.D. Effect of the state of the ground on the local heat balance. *Mon. Weather Rev.* **1958**, *86*, 171–176. [\[CrossRef\]](#)
- Ran, L.; Pleim, J.; Gilliam, R.; Binkowski, F.S.; Hogrefe, C.; Band, L. Improved meteorology from an updated wrf/cmaq modeling system with modis vegetation and albedo. *J. Geophys. Res. Atmos.* **2016**, *121*, 2393–2415. [\[CrossRef\]](#)
- Martilli, A. Current research and future challenges in urban mesoscale modelling. *Int. J. Climatol.* **2007**, *27*, 1909–1918. [\[CrossRef\]](#)
- Holt, T.; Pullen, J. Urban canopy modeling of the new york city metropolitan area: A comparison and validation of single- and multilayer parameterizations. *Mon. Weather Rev.* **2007**, *135*, 1906–1930. [\[CrossRef\]](#)
- Wang, Z.H.; Bou-Zeid, E.; Au, S.K.; Smith, J.A. Analyzing the sensitivity of wrf's single-layer urban canopy model to parameter uncertainty using advanced monte carlo simulation. *J. Appl. Meteorol. Climatol.* **2011**, *50*, 1795–1814. [\[CrossRef\]](#)

30. Mölders, N. On the uncertainty in mesoscale modeling caused by surface parameters. *Meteorol. Atmos. Phys.* **2001**, *76*, 119–141. [\[CrossRef\]](#)
31. Atkinson, B.W. Numerical modelling of urban heat-island intensity. *Bound. Layer Meteorol.* **2003**, *109*, 285–310. [\[CrossRef\]](#)
32. Nitis, T.; Tsegas, G.; Korres, G.; Douros, I.; Moussiopoulos, N. Influence of sea surface temperature variation on basic mesoscale flows over coastal areas. In Proceedings of the 10th International Conference on Environmental Science and Technology, Cos Island, Greece, 5–7 September 2007.
33. Shimada, S.; Ohsawa, T.; Kogaki, T.; Steinfeld, G.; Heinemann, D. Effects of sea surface temperature accuracy on offshore wind resource assessment using a mesoscale model. *Wind Energy* **2015**, *18*, 1839–1854. [\[CrossRef\]](#)
34. Hu, D.Y.; Yang, L.M.; Zhou, J.; Deng, L. Estimation of urban energy heat flux and anthropogenic heat discharge using aster image and meteorological data: Case study in beijing metropolitan area. *J. Appl. Remote Sens.* **2012**, *6*, 063559. [\[CrossRef\]](#)
35. Fan, H.L.; Sailor, D.J. Modeling the impacts of anthropogenic heating on the urban climate of philadelphia: A comparison of implementations in two pbl schemes. *Atmos. Environ.* **2005**, *39*, 73–84. [\[CrossRef\]](#)
36. Population Division, Department of Economic and Social Affairs, United Nations. *World Urbanization Prospects the 2011 Revision*; Population Division, Department of Economic and Social Affairs, United Nations: New York, NY, USA, 2012.
37. Nitis, T.; Tsegas, G.; Moussiopoulos, N.; Gounaridis, D. Assimilating anthropogenic heat flux estimated from satellite data in a mesoscale flow model. In *International Technical Meeting on Air Pollution Modelling and Its Application*; Clemens, M., George, K., Eds.; Springer: Crete, Greece, 2016; pp. 219–224.
38. Kunz, R.; Moussiopoulos, N. Simulation of the wind-field in athens using refined boundary-conditions. *Atmos. Environ.* **1995**, *29*, 3575–3591. [\[CrossRef\]](#)
39. Moussiopoulos, N.; Douros, I.; Tsegas, G.; Kleanthous, S.; Chourdakis, E. An air quality management system for policy support in cyprus. *Adv. Meteorol.* **2012**, *2012*, 959280. [\[CrossRef\]](#)
40. Büttner, G.; Feranec, J.; Jaffrain, G.; Mari, L.; Maucha, G.; Soukup, T. The corine land cover 2000 project. *EARSeL eProceedings* **2004**, *3*, 331–346.
41. Farr, T.G.; Rosen, P.A.; Caro, E.; Crippen, R.; Duren, R.; Hensley, S.; Kobrick, M.; Paller, M.; Rodriguez, E.; Roth, L.; et al. The shuttle radar topography mission. *Rev. Geophys.* **2007**, *45*. [\[CrossRef\]](#)
42. Yu, M.; Wu, B.; Yan, N.; Xing, Q.; Zhu, W. A method for estimating the aerodynamic roughness length with ndvi and brdf signatures using multi-temporal proba-v data. *Remote Sens.* **2017**, *9*, 6. [\[CrossRef\]](#)
43. Chen, Q.; Jia, L.; Hutjes, R.; Menenti, M. Estimation of aerodynamic roughness length over oasis in the heihe river basin by utilizing remote sensing and ground data. *Remote Sens.* **2015**, *7*, 3690–3709. [\[CrossRef\]](#)
44. Gupta, R.K.; Prasad, T.S.; Vijayan, D. Estimation of roughness length and sensible heat flux from wifs and noaa avhrr data. *Adv. Space Res.* **2002**, *29*, 33–38. [\[CrossRef\]](#)
45. Moran, M.S.; Clarke, T.R.; Inoue, Y.; Vidal, A. Estimating crop water deficit using the relation between surface-air temperature and spectral vegetation index. *Remote Sens. Environ.* **1994**, *49*, 246–263. [\[CrossRef\]](#)
46. Davidson, A.; Wang, S. The effects of sampling resolution on the surface albedos of dominant land cover types in the north american boreal region. *Remote Sens. Environ.* **2004**, *93*, 211–224. [\[CrossRef\]](#)
47. Wang, Z.; Zeng, X.; Barlage, M.; Dickinson, R.E.; Gao, F.; Schaaf, C.B. Using modis brdf and albedo data to evaluate global model land surface albedo. *J. Hydrometeorol.* **2004**, *5*, 3–14. [\[CrossRef\]](#)
48. Falasca, S.; Catalano, F.; Moroni, M. Numerical study of the daytime planetary boundary layer over an idealized urban area: Influence of surface properties, anthropogenic heat flux, and geostrophic wind intensity. *J. Appl. Meteorol. Climatol.* **2016**, *55*, 1021–1039. [\[CrossRef\]](#)
49. Nitis, T.; Tsegas, G.; Moussiopoulos, N.; Gounaridis, D.; Bliziotis, D. *Satellite Data Based Approach for the Estimation of Anthropogenic Heat Flux over Urban Areas*; SPIE: Bellingham, WA, USA, 2017; Volume 10444.
50. Willmott, C.J.; Robeson, S.M.; Matsuura, K. A refined index of model performance. *Int. J. Climatol.* **2012**, *32*, 2088–2094. [\[CrossRef\]](#)
51. Nitis, T.; Kitsiou, D.; Klač, Z.B.; Prtenjak, M.T.; Moussiopoulos, N. The effects of basic flow and topography on the development of the sea breeze over a complex coastal environment. *Q. J. R. Meteorol. Soc.* **2005**, *131*, 305–327. [\[CrossRef\]](#)
52. Mills, G.A.; Hayden, C.M. The use of high horizontal resolution satellite temperature and moisture profiles to initialize a mesoscale numerical weather prediction model—A severe weather event case study. *J. Appl. Meteorol. Climatol.* **1983**, *22*, 649–663. [\[CrossRef\]](#)
53. Draxler, R.R. The use of global and mesoscale meteorological model data to predict the transport and dispersion of tracer plumes over washington, d.c. *Weather Forecast* **2006**, *21*, 383–394. [\[CrossRef\]](#)
54. Schlünzen, K.H.; Sokhi, S.R. *Joint Report of Cost Action 728 and Gurme: Overview of Tools and Methods for Meteorological and Air Pollution Mesoscale Model Evaluation and User Training*; World Meteorological Organization (WMO): Geneva, Switzerland, 2008; Volume 181, p. 124.